Int. J. Electrochem. Sci., 7 **(2012)** 2304 - 2319

International Journal of
ELECTROCHEMICAL
SCIENCE
www.electrochemsci.org

Influence of the 2-Mercapto-1-Methyl Imidazole (MMI) on the Corrosion Inhibition of Mild Steel in 5% HCl

H. B. Ouici[1], *O. Benali*[1], *Y. Harek*[2], *S.S. Al-Deyab*[3], *L. Larabi*[2], *B. Hammouti*[4,*]

[1] Département de Biologie, Faculté des sciences et de la technologie, Université Tahar Moulay, Saïda, Algérie
[2] Département de Chimie, Faculté des Sciences, Université Abou Bekr Belkaïd, Tlemcen, Algérie
[3] Petrochemical Research Chair, Chemistry Department, College of Science, King Saud University, P.O. Box 2455, Riyadh 11451, Saudi Arabia
[4] Laboratoire de Chimie Appliquée et Environnement, Faculté des Sciences, Université Mohamed Premier, Oujda, Morocco
[*]E-mail: hammoutib@gmail.com

Received: 11 January 2012 / *Accepted:* 2 February 2012 / *Published:* 1 March 2012

Inhibitive performance of 2-Mercapto-1-Methyl Imidazole on corrosion behavior of mild steel in 5% HCl solution was investigated by means of weight loss, electrochemical measurements, SEM and EDX. The increase in concentration and immersion time shows a positive effect on inhibition efficiency, while temperature has a negative effect. Polarization curves reveal that MMI is a cathodic type inhibitor. Changes in impedance parameters were indicative of the formation of a protective film on the metal surface. The adsorption of MMI on mild steel surface obeys Langmuir adsorption isotherm. Some thermodynamic functions of dissolution and adsorption processes were also determined.

Keywords: Mild steel, EIS, Polarization, SEM, Acid corrosion

1. INTRODUCTION

Because of the general aggressiveness of acid solutions, the use of inhibitors to control the destructive attack of acid environment was found to have widespread applications in many industries [1]. Recently, the inhibition of steel corrosion in acid solutions by different types of organic inhibitors has been extensively studied [2–7]. Nitrogen-containing organic compounds are known to be efficient corrosion inhibitors in hydrochloric solutions, while sulfur- containing compounds are sometimes preferred for sulphuric solutions [8]. But the compounds containing nitrogen and sulfur are a good inhibitors in different medium [9-11]. The corrosion inhibition of mild steel is a subject of large-scale

technological importance, due to the fundamental economical implications of this material in the industrial medium [12-16]. Recently our research group has shown [17- 20] that 2-mercapto-1-methylimidazole (MMI) can be very useful corrosion inhibitor for steel and copper under acidic conditions. The latter gives rise to a considerable molecular adsorption of the MMI on the metal surface exposed to the aggressive solution. The present work is an extension of earlier works on the influence of the 2-mercapto-1-methylimidazole (MMI) on the inhibition of corrosion of mild steel in HCl 5%. The inhibition performance is evaluated by weight loss, Tafel polarization and electrochemical impedance spectroscopy (EIS). MEB and EDX have been applied to study the surface morphological features of the inhibitor adsorption.

2. EXPERIMENTAL DETAILS

2.1. Materials

Mild steel composed of (in wt.%) C ≤ 0.1%, Si≤ 0.03%, Mn≤ 0.2%, P≤ 0.02%, Cr≤ 0.05%, Ni≤ 0.05%, Al ≤0.03% and the remainder iron was used as the working electrode for all studies.

The inhibitor used is 2-mercapto-1-methylimidazole (Merck). The molecular structure of the inhibitor is as follows:

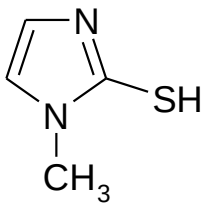

Figure 1. Molecular structures of 2-mercapto-1-methylimidazole (MMI)

The acid solutions were made from AR grade H_2SO_4. Appropriate concentration of acid was prepared by using distilled water.

2.2. Weight loss measurements

For the weight loss measurements, the experiments were carried out in solution of 5% HCl (uninhibited and inhibited) on mild steel. Sheets with dimensions 19.5 x 13.5 x 2 mm were used. They were polished successively with different grades of emery paper up 1200 grade. Each run was carried out in a glass vessel containing 50 ml test solution. A clean weight mild steel sample was completely immersed at an inclined position in the vessel. After 1 h of immersion in 5% HCl with and without addition of inhibitor at different concentrations, the specimen was withdrawn, rinsed with distilled water, washed with ethanol, dried and weighted. The weight loss was used to calculate the corrosion rate in milligrams per square centimeter per hour.

All experiments were carried out in freshly prepared solution at constant temperatures, 30, 40, 50°C and 60 ± 0.1 °C using a thermostat.

2.3. Electrochemical measurements

Electrochemical experiments were carried out in a glass cell (CEC/TH-Radiometer) with a capacity of 500 ml. A platinum electrode and a saturated calomel electrode (SCE) were used as a counter electrode and a reference electrode. The working electrode (WE) was in the form of a disc cut from mild steel under investigation and was embedded in a Teflon rod with an exposed area of 0.5 cm^2.

Electrochemical impedance spectroscopy (EIS), potentiodynamic and linear polarization were conducted in an electrochemical measurement system (VoltaLab40) which comprises a PGZ301 potentiostat, a personal computer and VoltaMaster 4 and Zview software. The potentiodynamic current–potential curves were recorded by changing the electrode potential automatically from –750 to –350 mV with scanning rate of 0.5 mV s^{-1}. The polarization resistance measurements were performed by applying a controlled potential scan over a small range typically 15 mV with respect to E_{corr}. The resulting current is linearly plotted versus potential, the slope of this plot at E_{corr} being the polarization resistance (Rp). All experiments were carried out in freshly prepared solution at 30°C. The ac impedance measurements were performed at corrosion potentials (E_{corr}) over a frequency range of 10 kHz–40 mHz, with a signal amplitude perturbation of 10 mV. Nyquist plots were obtained.

2.4. Scanning electron microscopy (SEM)

The carbon steel specimens before and after immersion were investigated by using a Quanta 200 FEI Company scanning electron microscope. The energy of the acceleration beam employed was 20 kV. The group is equipped with a system complete of microanalyse X (detector EDXEDAX) and with a detector of back-scattered electrons. This SEM allows giving the chemical composition of the sample.

3. RESULTS AND DISCUSSION

3.1. Weight loss measurements and electrochemical studies

The effect of addition of MMI tested at different concentrations on the corrosion of mild steel in 5% HCl solution was studied by weight loss measurements at 30 °C after 1 h of immersion period. From the values of corrosion rate in the absence (W_u) and presence (W_i) of inhibitor, the inhibition efficiency, E(%), was determined using the following equation:

$$P\ \% = \frac{W_u - W_i}{W_u} \times 100 \qquad (1)$$

It is obvious from the Table 1 that the MMI inhibit the corrosion of mild steel in 5% HCl solution at all concentrations used in this study and the corrosion rate (W) is seen to decrease continuously with increasing additive concentration at 30 °C. Indeed, corrosion rate values of mild steel decrease when the inhibitor concentration increases while P(%) values of MMI increase with the increase of the concentration, the maximum P(%) of 94% is achieved at $5x10^{-3}$ M. The inhibition of corrosion of mild steel by MMI can be explained in terms of adsorption on the metal surface. This compound can be adsorbed on the metal surface by the interaction between lone pairs of electrons of nitrogen and sulfur atoms of the inhibitor and the metal surface. This process is facilitated by the presence of vacant orbitals of low energy in iron atom, as observed in the transition group metals [17, 19].

Table 1. Corrosion parameters obtained from weight loss measurements for mild steel in 5% HCl containing various concentrations of MMI at 30 °C.

Conc. (Mol/L)	W (mg/cm^2.h)	P%
Blank	5.50	----
$5x10^{-4}$	0.80	85.45
10^{-3}	0.63	88.54
$2x10^{-3}$	0.50	91.00
$5x10^{-3}$	0.33	94.00

Polarization measurements have been carried out in order to gain knowledge concerning the kinetics of the anodic and cathodic reactions. Polarization curves of the mild steel in 5% HCl solutions without and with addition of different concentrations of MMI are shown in Fig. 2. The anodic and cathodic current–potential curves are extrapolated up to their intersection at a point where corrosion current density (I_{corr}) and corrosion potential (E_{corr}) are obtained [21]. Table 2 shows the electrochemical parameters (I_{corr}, E_{corr}, b_a and b_c) obtained from Tafel plots for the mild steel electrode in 5% HCl solution without and with different concentrations of MMI. The I_{corr} values were used to calculate the inhibition efficiency, P(%) (listed in Table 2), using the following equation :

$$P\% = \frac{I_u - I_i}{Iu} \times 100 \qquad (2)$$

where I_u and I_i are the corrosion current densities for mild steel electrode in the uninhibited and inhibited solutions, respectively.

From this figure, it can be seen that with the increase of MMI extract concentrations, both anodic and cathodic currents were inhibited. This result shows that the addition of MMI inhibitor reduces anodic dissolution and also retards the hydrogen evolution reaction.

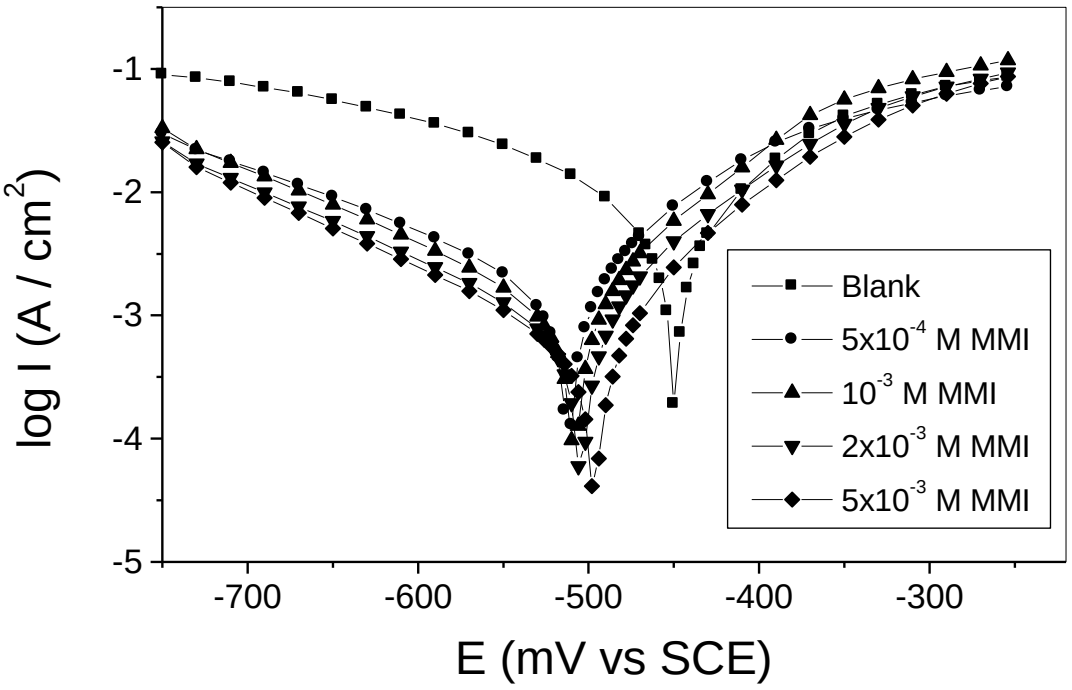

Figure 2. Polarisation curves of mild steel in 5% HCl at different concentrations of MMI at 30°C.

Table 2. Electrochemical parameters and the corresponding corrosion inhibition efficiencies for the corrosion of mild steel in 5% HCl containing different concentrations MMI at 30 °C.

Conc. (mol/L)	E_{corr} (mV*vs* CSE)	I_{corr} (mA/cm^2)	R_p (Ω.Cm^2)	$-b_c$ (mV/dec)	b_a (mV/dec)	P% (I_{corr})	P% (R_p)
Blank	-450	6.28	4.08	180	100	----	----
5x10^{-4}	-513	1.54	14.74	175	93	75.41	72.32
10^{-3}	-511	1.31	20.23	178	80	79.14	79.83
2x10^{-3}	-508	0.73	28.28	160	80	88.38	85.57
5x10^{-3}	-500	0.55	38.00	156	75	91.18	89.26

In addition, the parallel cathodic Tafel curves in Fig. 2 show that the hydrogen evolution is activation controlled and the reduction mechanism is not affected by the presence of the inhibitor [2]. The inspection of results in Table 2 indicate that MMI inhibits the corrosion process in the studied range of concentrations and P (%) increases with the concentration ofr the inhibitor, reaching its maximum value, 91.18%, at 5x10^{-3} M. The values of the cathodic Tafel lines, b_c, show slight changes with the addition of MMI. This result means that the mechanism at the electrode reaction is not changed [1, 2].

Impedance measurements of the mild steel electrode at its open circuit potential after 1 h of immersion in 5% HCl solution with and without MMI inhibitor were performed over the frequency range from 10 kHz to 40 mHz. Fig. 3 shows the obtained Nyquist plots of mild steel in 5% HCl

solution in the absence and presence of different concentrations of MMI. Inspections of these recorded spectra reveal that each impedance diagram consists of a large capacitive loop at high frequency (HF) with one capacitive time constant. As usually indicated in the EIS study, the HF capacitive loop is related to the charge transfer process of the metal corrosion and the double-layer behaviour [22].

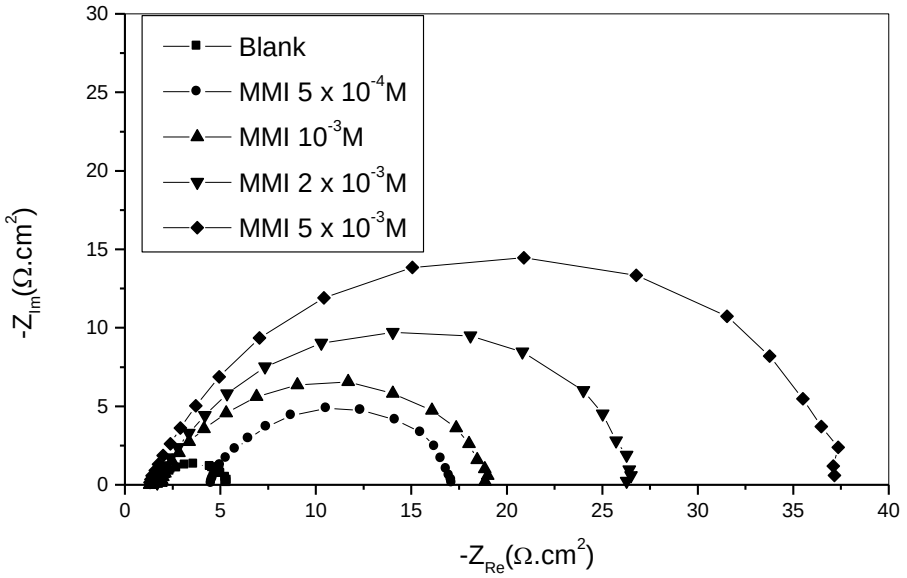

Figure 3. Complex plane plots for mild steel 5% HCl solution in the absence and in the presence of different concentrations of MMI at 30°C.

The circuit consists of a constant phase element (CPE) Q, in parallel with a resistor R_t The use of CPE-type impedance has been extensively described in [23-25]:

$$Z_{CPE} = [Q(jw)^n]^{-1} \quad (3)$$

The above equation provides information about the degree of non-ideality in capacitance behaviour. Its value makes it possible to differentiate between the behaviour of an ideal capacitor (n = 1) and of a CPE (n < 1).

Considering that a CPE may be considered as a parallel combination of a pure capacitor and a resistor that is inversely proportional to the angular frequency, the value of capacitance, C_{dl}, can thus be calculated for a parallel circuit composed of a CPE (Q) and a resistor (R_t), according to the following formula [26,27]:

$$Q = (C_{dl}R_t)^n/R_t \quad (4)$$

The impedance spectra of mild steel in 5% HCl with and without inhibitor were analysed by using the circuit in Fig. 4, and the double layer capacitance (C_{dl}) was calculated in terms of Eq. 5. Values of elements of the circuit corresponding to different corrosion systems, including values of C_{dl}, are listed in Table 3.

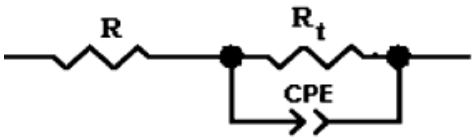

Figure 4. The equivalent circuit of the impedance spectra obtained for MMI.

The percent inhibition efficiency is calculated by charge transfer resistance obtained from Nyquist plots, according to the equation:

$$P\% = \frac{R_t' - R_t}{R_t'} \times 100 \qquad (5)$$

where R_t' and R_t are the charge transfer resistance values without and with inhibitor, respectively.

As can be seen from table 3, the increase in resistance in the presence of MMI compared to HCl alone is related to the corrosion protection effect of the phytochemical constituents. The value of C_{dl} decreases in the presence of MMI, suggesting that the MMI molecules function by adsorption at the metal solution/interface. It is important to point out that n reaches approximately the same value of 0.80. This result can be interpreted as an indication of the degree of heterogeneity of the metal surface, corresponding to a small depression of the double layer capacitance semicircle [28]. The values of inhibition's efficiency increase with inhibitor concentration at a maximum value (90.29%) at $5x10^{-3}$M.

Table 3. Impedance parameters and inhibition efficiency for the corrosion of mild steel in 5% HCl containing different of different concentrations of MMI at 30°C

Conc. (Mol/L)	Q ($s^n\Omega^{-1}.cm^{-2}$)	n	R_t ($\Omega.cm^2$)	C_{dl} (μ F cm^{-2})	P (%)
Blank	$4.2x10^{-4}$	0.83	3.60	111.06	-----
$5x10^{-4}$	$1.5x10^{-4}$	0.80	12.92	31.47	72.14
10^{-3}	$1.3x10^{-4}$	0.80	18.83	28.91	80.88
$2x10^{-3}$	$1.0x10^{-4}$	0.81	25.31	24.59	85.38
$5x10^{-3}$	$9.4x10^{-5}$	0.82	37.08	25.25	90.29

3.2. Effect of immersion time on corrosion of mild steel

In order to assess the stability of inhibitive behaviour of inhibitors on a time scale, weight loss measurements were performed in 5% HCl in absence and presence of MMI at $5x10^{-3}$M for different immersion time at temperature 303 K. Corrosion rates were plotted against immersion time as seen from Fig. 5.

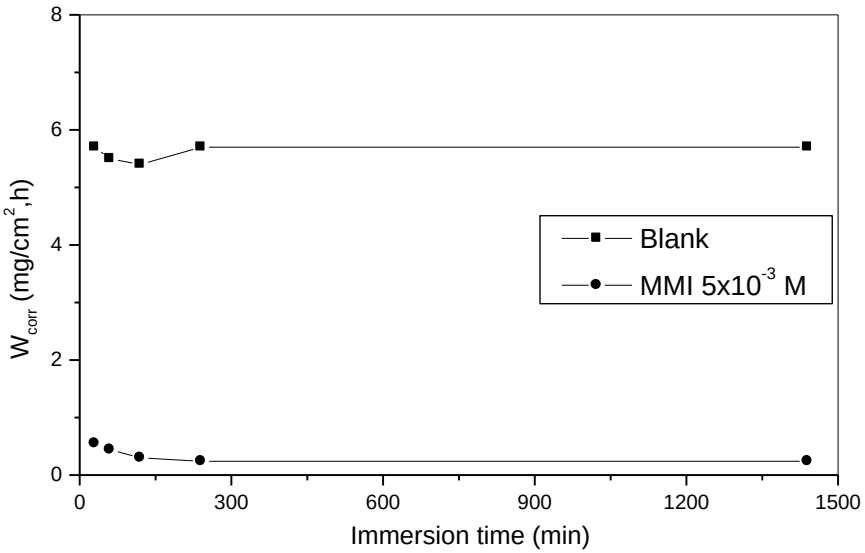

Figure 5. Effect of immersion time on corrosion rate for mild steel in 5% HCl at 30°C with and without of optimal concentration.

The Table 4 shows that the inhibition efficiency of MMI increased with immersion time and stabilized after 240 min. The increase in inhibition for MMI reflects this strong adsorption on the mild steel surface, resulting in a more protective layer. While, Shriver et al. [28] and Ishtiaque et al. [29] explained that decrease in inhibition for long period of immersion can be attributed to the depletion of available inhibitor molecules in the solution due to chelate formation between iron and the inhibitor ligands. From these observations, we can conclude that studied imidazole derivative is efficient corrosion inhibitor for mild steel in 5% hydrochloric acid solutions.

Table 4. Effect of immersion time on inhibitor performance for mild steel in 5% HCl at 30°C for the MMI at $5x10^{-3}$M

Immersion time (min)	P (%)
30	90.35
60	94.00
120	94.44
240	95.79
1440	95.79

3.3. Effect of temperature on corrosion of mild steel

The effect of temperature on the performance of MMI as corrosion inhibitor is investigated by weight loss measurements in the temperature range 303 – 333°C in absence and presence of MMI at

different concentrations. Table 5 shows values of corrosion rate (W_{corr}) and inhibition efficiency (P %) obtained from weight loss measurements at different temperatures.

Table 5. Values of corrosion rates and inhibition efficiency for different concentrations of MMI at various concentrations.

Temperature (°C)	Conc. (Mol/L)	W (mg/cm^2.h)	E_w (%)
	Blank	5.50	----
	5×10^{-4}	0.80	85.45
303	10^{-3}	0.63	88.54
	2×10^{-3}	0.50	91.00
	5×10^{-3}	0.33	94.00
	Blank	9.33	----
	5×10^{-4}	1.80	80.70
313	10^{-3}	1.21	87.00
	2×10^{-3}	0.87	90.70
	5×10^{-3}	0.70	92.50
	Blank	14.15	----
	5×10^{-4}	3.30	76.70
323	10^{-3}	2.55	82.00
	2×10^{-3}	1.72	87.84
	5×10^{-3}	1.30	90.81
	Blank	24.90	----
	5×10^{-4}	8.96	64.00
333	10^{-3}	4.64	81.36
	2×10^{-3}	3.52	85.86
	5×10^{-3}	2.97	88.07

Apparent activation energy for the corrosion process is calculated using Arrhenius Eq. (6) [29, 30]:

$$W_{corr} = A \exp(-E_a/RT) \quad (6)$$

where W_{corr} is the corrosion rate (obtained from weight loss measurements), k is the Arrhenius pre-exponential factor, E_a the apparent activation energy for corrosion process, R the universal gas constant and T the absolute temperature.

The E_a value corresponds to that of hydrogen ions activation and in fact can be considered as a verification of the cathodic control of the corrosion process [29, 31].

The apparent activation energies (E_a) and pre-exponential factor (A) at different concentrations of MMI are determined by linear regression between ln W_{corr} and 1/T (Fig. 6) and the results are listed in Table 6.

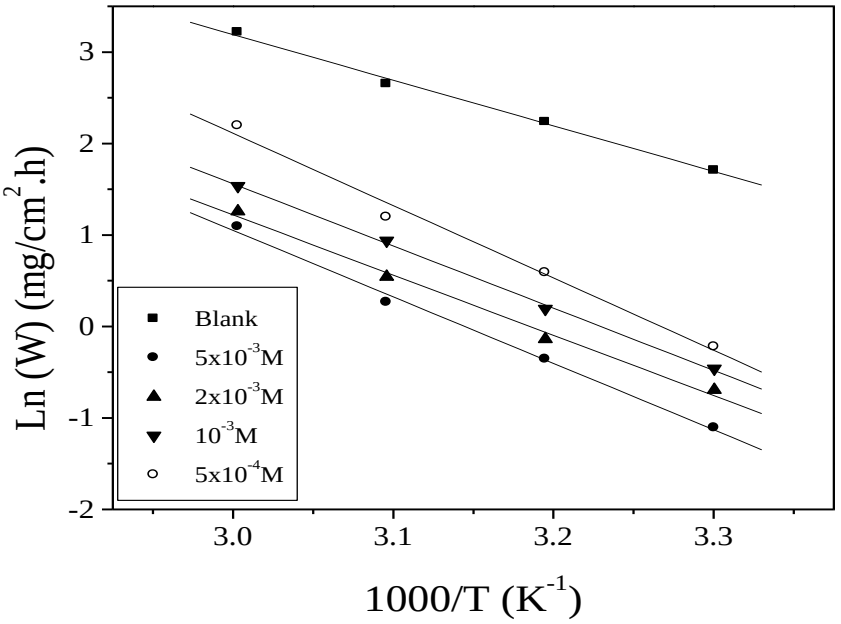

Figure 6. Arrhenius plots of steel in acid with and without different concentrations of MMI.

Kinetic parameters such as enthalpy and entropy of corrosion process may be evaluated from the temperature effect. An alternative formulation of Arrhenius equation is [32-34]:

$$W = \frac{RT}{Nh}\exp\left(\frac{\Delta S_{\mathrm{a}}^{O}}{R}\right)\exp\left(-\frac{\Delta H_{\mathrm{a}}^{O}}{RT}\right) \qquad (7)$$

Where h is plank's constant, N is Avogrado's number, $\Delta S°_a$ and $\Delta H°_a$ are the entropy and enthalpy of activation, respectively.

Straight lines are obtained with a slope ($-\Delta H°_a$ /R) and intercept (Ln R/Nh + $\Delta S°_a$ /R) from which the $\Delta H°_a$ and $\Delta S°_a$ values are calculated (Table 6 and Figure 7). The positive sign of the enthalpy ($\Delta H°_a$) reflects the endothermic nature of the copper dissolution process. The entropy of activation ΔS_a° in the absence of inhibitor is positive and this value increases positively with the MMI concentration. The increase of ΔS_a° implies that an increase in disordering takes place on going from reactants to the activated complex [34]. All the linear regression coefficients are close to one, indicating that the corrosion of mild steel in 5% HCl solution may be elucidated using the kinetic model. Table 6 shows that the values of E_a for inhibited solution are higher (54.71– 65.71 kJ mol^{-1}) than that for uninhibited solution (41.45 kJ mol^{-1}). The values of A in the presence of MMI are higher than that in uninhibited solution. It is clear from Eq. (6) that the higher E_a and the lower A lead to the lower corrosion rate. In general, the effect of E_a on mild steel corrosion is larger than that of A on mild steel corrosion. In the present study, values of E_a and A vary in similar manner and therefore, the combined effect of E_a and A results in increase of corrosion rate with temperature. The same behaviour has been reported by Ahamad at al. [35].

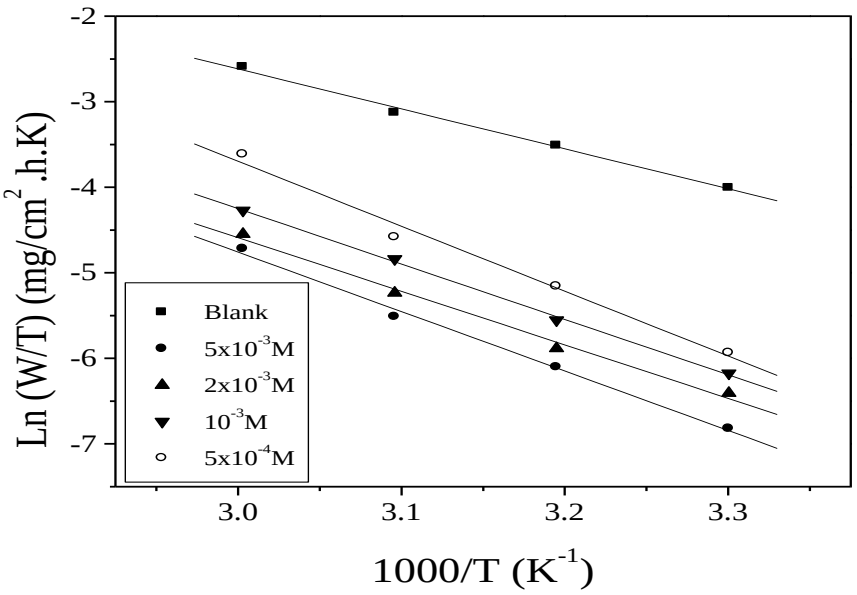

Figure 7. The relationship between Ln(W/T) and T^{-1} for different concentrations of MMI.

Table 6. The values of activation parameters for steel in5% HCl in the absence and the presence of different concentrations of MMI.

Conc. (Mol/L)	Pre-exponential factor (mg/cm^2.h)	Linear regression coefficient (r)	E_a (kJ/mol)	ΔH_a° (J/mol)	ΔS_a° (J/mol.K)
Blank	7.6275×10^{7}	0.99765	41.45	38.82	-102.85
5×10^{-4}	1.6632×10^{11}	0.99386	65.75	63.11	-38.94
10^{-3}	3.3961×10^{9}	0.99929	56.49	53.86	-71.29
2×10^{-3}	1.2701×10^{9}	0.99640	54.71	52.07	-79.47
5×10^{-3}	8.3958×10^{9}	0.99761	60.41	57.78	-63.77

3.4. Adsorption consideration

It is known that the adsorption isotherms are very important for the understanding of the mechanism of corrosion inhibition [36, 37]. The most frequently used isotherms are Langmuir, Freundlich, Temkin, Frumkin, etc. Assuming a direct relationship between inhibition efficiency and surface coverage, θ, of the inhibitor, weight loss measurements data were used to evaluate the surface coverage values, which are given by Eq. 8:

$$\theta = \frac{W_u - W_i}{W_u} \qquad (8)$$

where W_u and W_i are the corrosion rate values without and with inhibitor, respectively.

The θ values for different inhibitor concentrations at different temperature were tested by fitting to various isotherms. By far the best fit was obtained with the Langmiur isotherm. According to this isotherm θ is related to concentration inhibitor C via eq. 9:

$$\frac{C}{\theta} = \frac{1}{K} + C \quad \text{with} \qquad K = \frac{1}{55{,}5}\exp\left(-\frac{\Delta G^{0}_{ads}}{RT}\right) \tag{9}$$

where K is the adsorptive equilibrium constant and $\Delta G°_{ads}$ the free energy of adsorption**.**

The plots of C/ θ versus C (Fig. 8) yielded straight lines for all temperatures with slopes close to 1. This result indicates that the adsorption of compound under consideration on mild steel / acidic solution interface at all temperatures follows the Langmuir adsorption isotherm.

Thermodynamic parameters are important to study the inhibitive mechanism. The values of $\Delta G°_{ads}$ at different temperatures were estimated from the values of K and equation (9).

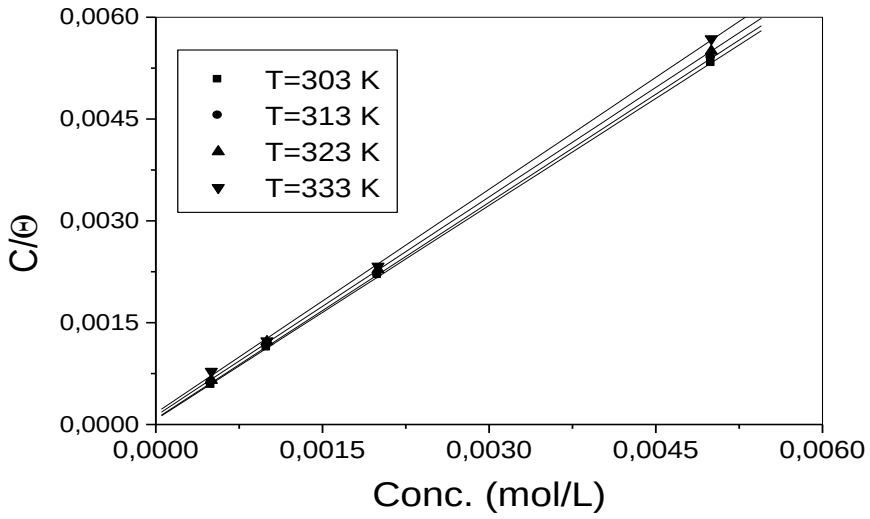

Figure 8. Langmuir's isotherms adsorption of MMI on the mild steel surface in 5% HCl at different temperatures.

The obtained values of K, slope, Regression factors and $\Delta G°_{ads}$ are summarized in table 7.

Table 7. The thermodynamic parameters for of mild steel in 5% HCl in the absence and presence of different concentrations of MMI.

T (K)	K (L/mol)	slope	r	$\Delta G°_{ads}$ (kJ/ mol)
303	$1.17x\ 10^4$	1.05	0.999	-33.72
313	$1.18x\ 10^4$	1.06	0.999	-34.85
323	$8.34x10^3$	1.07	0.999	-35.04
333	$5.88x\ 10^3$	1.09	0.999	-35.15

It can be seen that the values of the free enthalpy of adsorption are around -35 kJ / mol. The large negative of $\Delta G°_{ads}$ indicates that MMI is strongly adsorbed on the steel surface. MMI may adsorbed on a metal surface in the form of a neutral molecule via the chimisorption mechanism [17] involving the sharing of electrons between the nitrogen, sulphur atom and iron. The second mode (physisorption) is possible if one examines also the activation energy that increases in the presence of MMI. Adsorption of MMI can also occur through π electron interactions between the imidazole group structure of molecule and the metal surface. This is may be due to the availabilty of more sites on the metal surface in HCl solution because of the lesser adsorption of the chloride ions on the steel surface [19]. Therefore, we may suggest that the adsorption may occur through the lone pairs of heteroatoms and π electrons of the MMI molecules which outweigh the adsorption due to the cationic form of the MMI molecule on the metal surface. We can conclude that adsorption acts simultaneously by chemisorptions and physical adsorption [34]

3.5. Scanning electron microscopy (SEM)

The SEM is used here for the observation, in imaging by secondary electrons, of the topography of the sample. The elementary analysis is obtained by coupling the system with a dispersive analysis in energy (EDX). Our observations in the SEM concerned samples of carbon steel after 12 hours of immersion in 30°C in only 5% HCl (Fig. 9b), and with addition of $5x10^{-3}$M of the MMI (Fig. 9e). We observed on the surface the black spots corresponding to the stings of corrosion, as well as grey and white zones which they, correspond to the dandruff of iron oxides [38].

The analysis EDX of the surface reveals the presence of oxygen and iron, suggesting therefore the presence of iron oxide / hydroxide. On the figure 9e we remark the presence of the peaks of carbon, nitrogen, and sulfur is explained by the adsorption of the MMI on the products of corrosion of the steel.

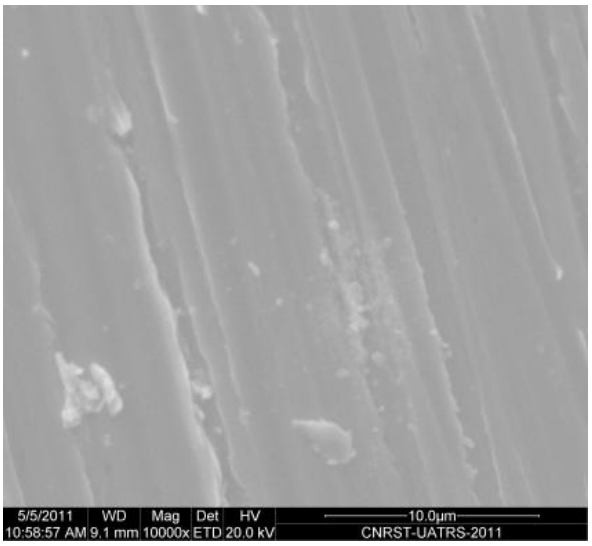

A

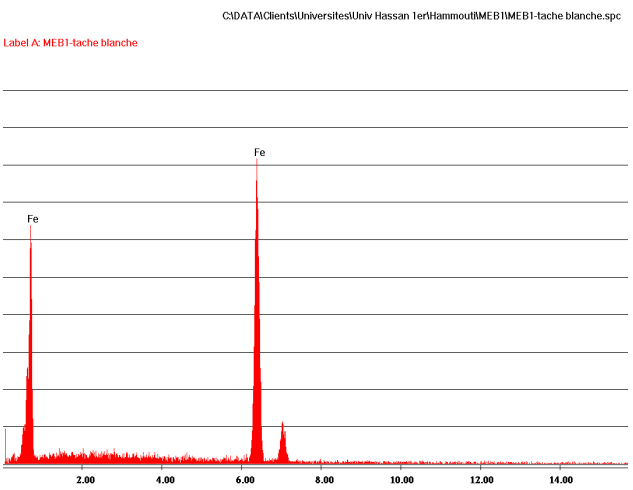

B

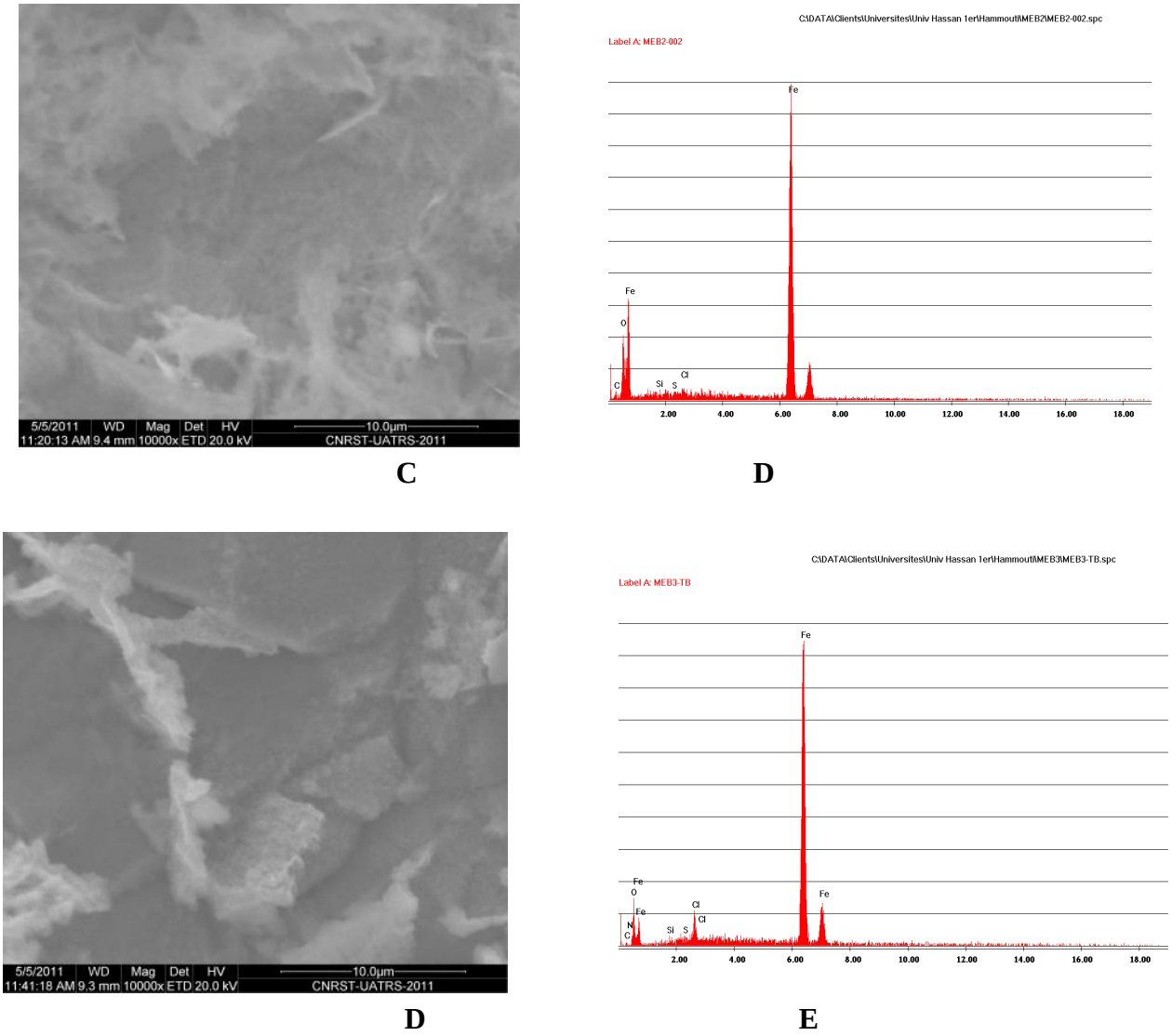

Figure 9. SEM observation and EDX analysis of the carbon steel surface after 12 h of immersion in 5% HCl: (a, b) without immersion, (c ,d) in 5% HCl alone and (d, e) in the presence of 5x 10^{-3}M of the MMI.

4. CONCLUSIONS

The main conclusions drawn from this study are:

- MMI inhibit the corrosion of mild steel in 5% HCl even at low concentrations.
- The inhibiting effect of MMI increases with increase of inhibitor concentration.
- The inhibition is due to adsorption of the inhibitor molecules on the steel surface and blocking its active sites.
- Adsorption of the inhibitors fits a modified Langmuir isotherm model.
- The analysis of the experimental data leads to the suggestion of chemisorption of the inhibitor on the metal surface. In fact, the apparent activation energy of the corrosion that is higher in

presence of MMI than in its absence and the higher values of the free energy of adsorption verify the chemisorptive character of the adsorption.

- The substance is adsorbed with the heteroatoms forming donor–acceptor bonds between unpaired electrons of the heteroatoms and the active centers of the metal surface.
- SEM and EDX examinations of the electrode surface confirmed the existence of such adsorbed film.

ACKNOWLEDGEMENTS
Prof S. S. Al-Deyab and Prof B. Hammouti extend their appreciation to the Deanship of Scientific Research at king Saud University for funding the work through the research group project.

References

1. H. El Attari, L. El Kadi, M. Lebrini, M. Traisnel, M. Lagrenee, *Corros. Sci*. 51 (2009) 1628.
2. F. Bentiss, M. Bouanis, B. Mernari, M. Traisnel, H. Vezin, M. Lagrenee, *Appl. Surf. Sci.* 253 (2007) 3696.
3. M.A. Amin, S.S. Abd El-Rehim, E.E.F. El-Sherbini, R.S. Bayyomi, *Electrochim. Acta* 52 (2007) 3588.
4. M.S. Abdelaal, M.S. Morad, *Br. Corros. J.* 36 (2001) 253.
5. A.M. Abdel-Gabar, B.A. Abd-El-Nabey, I.M. Sidahmed, A.M. El-Zayady, M. Saadawy, *Corros. Sci.* 48 (2006) 2765.
6. P. Bommersbach, C. Alemany-Dumont, J.P. Millet, B. Normand, *Electrochim.Acta* 51 (2005) 1076.
7. M.A. Quraishi, J. Rawat, *Mater. Chem. Phys.* 77 (2002) 43.
8. M. Lagrenee, B. Mernari, M. Bouanis, M. Taisnel, F. Bentiss, *Corros. Sci.* 44 (2002) 573.
9. O. Benali , L. Larabi , S. Merah , Y. Harek, *J. Mater. Environ. Sci.* 2 (1) (2011) 39-48.
10. L. Larabi, Y. Harek, O. Benali, S. Ghalem, *Prog. Org. Coat* 54 (2005) 256.
11. L. Larabi, , O. Benali, Y. Harek, *Port. Electrochim. Acta* 24 (2006) 337.
12. L. Herrag, B. Hammouti, S. Elkadiri, A. Aouniti, C. Jama, H. Vezin, F. Bentiss, *Corros. Sci*. 52 (2010) 3042.
13. S. Kharchouf, L. Majidi, M. Bouklah, B. Hammouti, A. Bouyanzer, A. Aouniti, *Arab. J. Chem*., doi:10.1016/j.arabjc.2010.12.002.
14. M. Benabdellah, A. Tounsi, K.F. Khaled, B. Hammouti, *Arab. J. Chem.* 4 (2011)17.
15. Q. Qu, Z. Hao, L. Li, W. Bai, Y. Liu, Z. Ding, *Corros.. Sci.* 51 (2009) 569.
16. S. M. A. Hosseini, A. Azimi, *Corros. Sci.* 51 (2009) 728.
17. O. Benali, L. Larabi, B. Tabti , Y. Harek, *Anti-Corros. Met. and Mat*. 52 (2005) 280.
18. L. Larabi, O. Benali, S. M. Mekelleche, Y. Harek, *Appl. Surf. Sci*. 253 (2006) 1371.
19. O. Benali, L. Larabi, M. Traisnel , L. Gengenbre, Y. Harek, *Appl. Surf. Sci.* 253 (2007) 6130.
20. O. Benali, L. Larabi, Y. Harek, *J. Saudi Chem. Soc.* 14 (2010) 231.
21. S.S. Abd EI-Rehim, M.A.M. Ibrahim, K.F. Khaled, *J. Appl. Electrochem*. 29 (1999) 593.
22. M.S. Morad, *Corros. Sci*. 42 (2000) 1307.
23. M. Hukovic-Metikos, R. Babic, Z. Grutac, *J. Appl. Electrochem.* 32 (2002) 35.
24. F. Mansfeld, *Corrosion* 37 (1981) 301.
25. E. Mccafferty, Corros. Sci. 39 (1997) 243.
26. X. Wu, H. Ma, S. Chen, Z. Xu, A. Sui, *J. Electrochem. Soc*. 146 (1999) 1847.
27. H. Ma, S. Chen, B. Yin, S. Zhao, X. Liu, *Corros. Sci.* 45 (2003) 867.

28. D.F. Shriver, P.W. Atkins, C.H. Langford, Inorganic Chemistry, second ed.,Oxford University Press, Oxford, 1994. pp. 238.
29. Ishtiaque Ahamad, Rajendra Prasad, M.A. Quraishi, *Corros. Sci.* 52 (2010) 1472.
30. Benali Omar, Ouazene Mokhtar , *Arab. J. Chem.* 4 (2011) 443.
31. N.P. Zhuk, Course on Corrosion and Metal Protection, Metallurgy, Moscow, 1976.
32. M. Benabdellah, A. Tounsi, K.F. Khaled. B. Hammouti, *Arab. J. Chem*, 4 (2011) 17-24.
33. Elouali I., Hammouti B., Aouniti A., Ramli Y., Azougagh M., Essassi E.M., Bouachrine M. *J. Mater. Environ. Sci.* 1 (2010) 1.
34. M. Dahmani, A. Et-Touhami, S.S. Al-Deyab , B. Hammouti, A. Bouyanzer, *Int. J. Electrochem. Sci.* 5 (2010) 1060.
35. I. Ahamad, R. Prasad, M.A. Quraishi, *Corros. Sci.* 52 (2010) 1472.
36. Hackerman N, Mccafferty E (1974) In: Proceedings of the fifth international congress on metallic corrosion. Houston, TX, p 542
37. O. Benali, L. Larabi, S. M. Mekelleche, Y. Harek , *J. Mater. Sci.* 41 (2006) 7064.
38. N. Labjar, S. El Hajjaji, M. Lebrini, M. Serghini Idrissi, C. Jama, F. Bentiss, *J. Mater. Environ. Sci.* 2 (2011) 309.